

Least Restrictive Hyperplane Control Barrier Functions

Mattias Trende and Petter Ögren

Abstract—Control Barrier Functions (CBFs) can provide provable safety guarantees for dynamic systems. However, finding a valid CBF for a system of interest is often non-trivial, especially for systems having low computational resources, higher-order dynamics, and moving close to obstacles of complex shape. A common solution to this problem is to use a purely distance-based CBF. In this paper, we study Hyperplane CBFs (H-CBFs), where a hyperplane separates the agent from the obstacle. First, we note that the common distance-based CBF is a special case of an H-CBF where the hyperplane is a supporting hyperplane of the obstacle that is orthogonal to a line between the agent and the obstacle. Then we show that a less conservative CBF can be found by optimising over the orientation of the supporting hyperplane, in order to find the Least Restrictive Hyperplane CBF. This enables us to maintain the safety guarantees while allowing controls that are closer to the desired ones, especially when moving fast and passing close to obstacles. We illustrate the approach on a double integrator dynamical system with acceleration constraints, moving through a group of arbitrarily shaped static and moving obstacles.

I. INTRODUCTION

Safety is crucial for many robotic systems, whether they are fully autonomous or include humans-in-the-loop. Over the last two decades, Control Barrier Functions (CBFs) have gained popularity as a means to ensure safety in robotics [1]–[3]. The role of a CBF is typically to serve as a safety filter. Given the state, the CBF can provide a set of safe control actions, and given a desired control action and a CBF, one can determine the safe control action that is closest to the desired one.

The difficult part of using CBFs to ensure safety is often to find a valid CBF [4]. For low-dimensional systems with simple obstacle geometries, it is often possible to derive a CBF analytically [5], but for more complex geometries and higher-dimensional systems, a closed-form solution might be quite conservative, while numerical solutions scale poorly with the increasing complexity [4]. A common solution to this problem is to utilise some type of approximate CBF. While there are machine learning approaches to the problem [6], using a black box model to guarantee safety can create additional challenges.

A very popular, but conservative, approach is the distance-based CBF, used in e.g., [7]–[11]. The key idea is to keep track of the distance to the closest part of the obstacle, and make sure it stays positive. It turns out that the distance-based CBF is equivalent to positioning a supporting hyperplane

The authors are with the Robotics, Perception and Learning Lab., School of Electrical Engineering and Computer Science, Royal Institute of Technology (KTH), SE-100 44 Stockholm, Sweden, {mtrende, petter}@kth.se

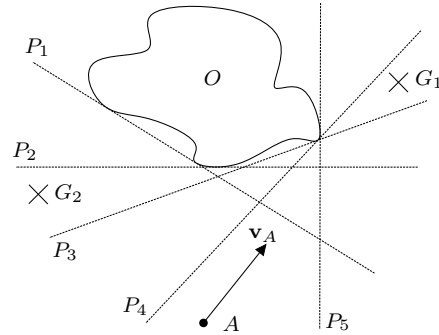


Fig. 1. An agent A with velocity \mathbf{v}_A in front of a general obstacle O . Five of the infinitely many supporting hyperplanes, parameterised by some θ , are shown ($P_1 - P_5$). Note that P_5 is an invalid choice of hyperplane for a CBF, as the agent and the obstacle are on the same side of the hyperplane. If the goal is at G_1 , an H-CBF based on P_4 is the least restrictive, whereas if the goal is at G_2 , an H-CBF based on P_1 or P_2 might be the least restrictive. The key idea in this paper is that given the desired action of the agent \mathbf{u}_{des} we optimise over a family of CBFs using θ , to find the least restrictive H-CBF, allowing a safe control \mathbf{u} that is as close as possible to \mathbf{u}_{des} .

at the closest point of the obstacle, orthogonal to the line between the obstacle and the agent, and applying a CBF that guarantees that the agent stays on the right side of this hyperplane. We call this method the Orthogonal Hyperplane-CBF (OH-CBF), and the more general approach of using any supporting plane a Hyperplane-CBF (H-CBF).

By using an H-CBF, the problem dimensionality is essentially reduced by projecting the system’s movement orthogonally to the plane [7]. This enables the use of an analytically derived one-dimensional CBF for higher-dimensional systems to guarantee safety. By properly choosing the hyperplane, you can handle a large set of obstacle geometries, such as ellipses and polygons [7], [10], [12]. The downside of using hyperplanes to describe obstacles is that it can be quite conservative, significantly restricting the motion of the vehicle close to the obstacle. However, in this paper, we note that conservativeness is only a problem if it prevents the agent from doing what it wants. Thus, we propose to find *the least restrictive H-CBF* as follows.

First, we note that the standard CBF approach [3] involves *first* choosing a CBF, and *then*, at each timestep, given a desired (possibly non-safe) control \mathbf{u}_{des} , finding a safe control \mathbf{u} that minimises $\|\mathbf{u} - \mathbf{u}_{des}\|$.

Then, the key part of the proposed approach is that instead of picking a single CBF, we pick a family of CBFs, parameterised by some θ , and then, in each time step, pick the individual CBF from the family that enables the smallest

deviation from \mathbf{u}_{des} , i.e., the combined choice of (θ, \mathbf{u}) that makes \mathbf{u} safe, and minimises $\|\mathbf{u} - \mathbf{u}_{\text{des}}\|$. We call this approach the *Least Restrictive Hyperplane CBF* (LRH-CBF).

An illustration of the approach is provided in Figure 1. The dashed lines represent different choices of θ . Now, imagine that the agent needs to go to G_1 , then the H-CBF corresponding to P_4 might be best, while if the destination is at G_2 , P_4 would be a very restrictive choice. Note also that P_2 corresponds to the minimum distance OH-CBF, which will most likely force the agent to brake, even though it is not on a collision course with the obstacle.

Thus, the main contribution of this paper is a generalisation of the distance-based CBF approach from [7]–[11], in which, instead of choosing an OH-CBF, we choose the LRH-CBF with respect to the desired control action, thereby minimising the difference between the chosen safe control and the desired control, making the approach less conservative. We also investigate how performance and computational requirements depend on the size of the family of hyperplanes we optimise over. Since the popular OH-CBF is a special case of LRH-CBF, it turns out that the computational complexity is comparable, but the performance is significantly better.

In the remainder of this paper, Section II looks further into the connections to previous work, while Section III summarises the theory of CBFs as well as the double integrator model with a corresponding H-CBF. Then, Section IV describes the proposed approach. Finally, the simulation results are presented in Section V, and the paper is concluded in Section VI.

II. RELATED WORK

There has been extensive work on CBFs for different representations of obstacles. The four most common ways are circles [7], [8], ellipses [10], [13], polygons [14]–[18], and hyperplanes [7], [8], [10], [12], [19]–[21]. In the last category, we also include the common CBF approach that tracks the distance from the agent to the closest point on an obstacle and ensures this distance remains positive [7], [19], [21]. Note that even though this approach does not explicitly mention hyperplanes, it is equivalent to an H-CBF touching the closest point of the obstacle, with a normal vector pointing towards the agent. Throughout the paper, we refer to these H-CBFs as *Orthogonal* (OH-CBFs), as they are orthogonal to the line between the agent and the closest point on the obstacle.

There are other works suggesting different orientations of H-CBFs. In [10], ellipsoidal bodies are considered, and the orientation of the hyperplane is chosen to maximise the distance between the hyperplane and the other nearby ellipsoid. In [20], the orientation of the H-CBF was chosen based on velocity obstacles (VO). They consider a second-order dynamic system, but in order to avoid having to work with higher-order CBFs, they create the CBFs in velocity space, aligned with the VOs. Finally, [12] picks H-CBFs based on a safe convex polytope, generated from free space in an occupancy grid map.

We also note that our use of H-CBFs makes the proposed approach suitable for combinations with several other methods in the literature, such as work on multi-agent systems [8], [22], [23], cooperative/neutral/adversarial obstacles [7], [24] and MPC [13], [25].

Finally, we note that this paper is different from all the approaches mentioned above in the sense that the choice of the H-CBF is dependent on the desired control. With a given desired control \mathbf{u}_{des} , we jointly optimise over the CBF family θ and the safe control \mathbf{u} to minimise $\|\mathbf{u} - \mathbf{u}_{\text{des}}\|$. Thus, it finds the LRH-CBF, in terms of enabling a safe control as close as possible to the desired control. None of the other papers considers the desired control when choosing the CBF, instead, they base it purely on the current state.

III. BACKGROUND

In this section, we first review some results from convex analysis, then summarise continuous and discrete CBF theory, followed by a description of a double integrator model and a common H-CBF for it.

A. Convex Analysis

Definition 1: A supporting hyperplane to a set $S \subset \mathbb{R}^n$ at a point $\mathbf{x}_0 \in \partial S$ (the boundary of S) is a hyperplane that passes through the point \mathbf{x}_0 and leaves the entire set on one side of the hyperplane (or on the hyperplane itself).

Theorem 1 (Supporting Hyperplane in Every Direction): If a set $S \subset \mathbb{R}^n$ is closed, convex, bounded, and has nonempty interior, then for every nonzero direction $\mathbf{n} \in \mathbb{R}^n$ there exists a point $\mathbf{p}^* \in S$ such that

$$\mathbf{n}^T \mathbf{p}^* = \max_{\mathbf{p} \in S} \mathbf{n}^T \mathbf{p} \quad (1)$$

and the hyperplane $\{\mathbf{p} : \mathbf{n}^T \mathbf{p} = \mathbf{n}^T \mathbf{p}^*\}$ supports S at \mathbf{p}^* .

Proof: See [26]. ■

Theorem 2 (Separating Hyperplane): Let $C_1, C_2 \subset \mathbb{R}^n$ be two compact, convex, nonempty, disjoint sets. Then, there exists a separating hyperplane $\mathbf{a}^T \mathbf{p} = b$, such that

$$\mathbf{a}^T \mathbf{p} \leq b \quad \forall \mathbf{p} \in C_1 \quad (2)$$

$$\mathbf{a}^T \mathbf{p} \geq b \quad \forall \mathbf{p} \in C_2. \quad (3)$$

Proof: See [26]. ■

B. Control Barrier Functions

Following the CBF definition in [3], consider a nonlinear affine control system in the form $\dot{\mathbf{x}} = \mathbf{f}(\mathbf{x}) + \mathbf{g}(\mathbf{x})\mathbf{u}$, where \mathbf{f} and \mathbf{g} are locally Lipschitz, $\mathbf{x} \in \mathbb{R}^n$ is the system state, and $\mathbf{u} \in \mathbb{R}^m$ is the system input. Then introduce the safe set \mathcal{C} , defined such that for every state $\mathbf{x}(t) \in \mathcal{C}$ there exists a permissible control $\mathbf{u} \in \mathcal{U}$ that ensures $\mathbf{x}(t + \epsilon) \in \mathcal{C}$ for all $\epsilon > 0$. Consider a continuously differentiable function $h : \mathbb{R}^n \rightarrow \mathbb{R}$. If h is such that $h(\mathbf{x}) \geq 0 \iff \mathbf{x} \in \mathcal{C}$ and satisfies the inequality

$$\sup_{\mathbf{u}} \dot{h}(\mathbf{x}, \mathbf{u}) \geq -\alpha(h(\mathbf{x})), \quad (4)$$

then h is a CBF. Here $\alpha : \mathbb{R} \rightarrow \mathbb{R}$ is an extended class \mathcal{K}_∞ function. This defines α to be a strictly increasing function that satisfies $\alpha(0) = 0$ and $\lim_{x \rightarrow \pm\infty} \alpha(x) = \pm\infty$.

Given a desired control \mathbf{u}_{des} , the search for a safe control \mathbf{u} close to the desired one can be formalised in the following optimisation problem [3]:

Problem 1 (CBF-QP):

$$\mathbf{u}(\mathbf{x}) = \underset{\mathbf{u}}{\operatorname{argmin}} (\mathbf{u} - \mathbf{u}_{\text{des}})^T \mathbf{Q} (\mathbf{u} - \mathbf{u}_{\text{des}}) \quad (5)$$

$$\text{s.t. } \dot{h}(\mathbf{x}, \mathbf{u}) \geq -\alpha(h(\mathbf{x})) \quad (6)$$

$$\mathbf{u} \in \mathcal{U}, \quad (7)$$

where Q is a positive definite matrix.

It can be shown that if the dynamics are as above, and $\mathcal{U} = \mathbb{R}^m$, the problem above is indeed a Quadratic Programming problem (QP) that is easy to solve [3].

C. Discrete Control Barrier Functions

When implementing CBFs on discrete-time systems, such as systems with modern embedded electronics, the CBF needs to be discretised into a Discrete-CBF (D-CBF) [27]. Instead of resulting in a QP for nonlinear affine systems, the problem becomes a Quadratically Constrained QP (QCQP).

Problem 2 (D-CBF-QCQP):

$$\mathbf{u}(\mathbf{x}) = \underset{\mathbf{u}}{\operatorname{argmin}} (\mathbf{u} - \mathbf{u}_{\text{des}})^T \mathbf{Q} (\mathbf{u} - \mathbf{u}_{\text{des}}) \quad (8)$$

$$\text{s.t. } \Delta h(\mathbf{x}_{k+1}, \mathbf{u}_k) \geq -\gamma h(\mathbf{x}_k) \quad (9)$$

$$\gamma \in (0, 1] \quad (10)$$

$$\mathbf{u} \in \mathcal{U}, \quad (11)$$

where Q is a positive definite matrix, the difference is $\Delta h(\mathbf{x}_{k+1}) = h(\mathbf{x}_{k+1}) - h(\mathbf{x}_k)$, and the discrete dynamics follow $\mathbf{x}_{k+1} = \mathbf{f}(\mathbf{x}_k) + \mathbf{g}(\mathbf{x}_k)\mathbf{u}_k$. This means that the constraint in (9) can be rewritten as

$$h(\mathbf{x}_{k+1}) \geq (1 - \gamma)h(\mathbf{x}_k). \quad (12)$$

D. Double Integrator Model

In this paper, we consider a double-integrator dynamic model subject to acceleration constraints. Let the state be $\mathbf{x} = (\mathbf{p}, \mathbf{v}) \in \mathbb{R}^4$ and $\dot{\mathbf{p}} = \mathbf{v}$, $\dot{\mathbf{v}} = \mathbf{u}$ with the acceleration constraint $\|\mathbf{u}\| \leq u_{\text{max}}$. Then the system can be written in control-affine form for the proper choice of \mathbf{f}, \mathbf{g} .

E. An H-CBF for the Double Integrator

For the double integrator model above, an H-CBF for an agent $(\mathbf{p}_A, \mathbf{v}_A)$ and a (possibly moving) obstacle $(\mathbf{p}_O, \mathbf{v}_O)$ is given in [7] as

$$h(\mathbf{x}) = \hat{\mathbf{n}}(\theta)^T (\mathbf{p}_A - \mathbf{p}_O) - \delta(\theta) - b. \quad (13)$$

Above, $\hat{\mathbf{n}}(\theta)$ is the unit normal vector of the hyperplane, $\delta(\theta)$ is the required safety margin between agent center \mathbf{p}_A and the obstacle center \mathbf{p}_O (with θ -dependence for non disc obstacles), and b is the braking distance needed for the agent to accelerate/retardate to the relative velocity of zero compared to the obstacle. The braking distance is given by

$$b = \begin{cases} \frac{(\hat{\mathbf{n}}(\theta)^T (\mathbf{v}_A - \mathbf{v}_O))^2}{2u_{\text{max}}}, & \text{for } \hat{\mathbf{n}}(\theta)^T (\mathbf{v}_A - \mathbf{v}_O) < 0 \\ 0, & \text{for } \hat{\mathbf{n}}(\theta)^T (\mathbf{v}_A - \mathbf{v}_O) \geq 0 \end{cases}, \quad (14)$$

since no braking is needed when the agent and obstacle are moving away from each other.

Note that above we have made a slight generalisation compared to [7], as they had no θ -dependency and instead used $\hat{\mathbf{n}}(\theta) = \hat{\mathbf{n}}_{AO}$, the direction from agent to obstacle, and $\delta(\theta) = \delta$.

Finally, we note that the derivative of h with respect to time, as needed in (6), in the case $b \neq 0$ is

$$\begin{aligned} \dot{h}(\mathbf{x}, \theta, \mathbf{u}) &= \nabla h(\mathbf{x}, \theta) \dot{\mathbf{x}} \\ &= \hat{\mathbf{n}}(\theta)^T (\mathbf{v}_A - \mathbf{v}_O - \mathbf{u} \frac{\hat{\mathbf{n}}(\theta)^T (\mathbf{v}_A - \mathbf{v}_O)}{u_{\text{max}}}). \end{aligned} \quad (15)$$

IV. PROPOSED APPROACH

In this section, we describe the proposed approach, show that it is a generalisation of the OH-CBF, discuss the existence and conservativeness of H-CBFs, investigate how to parameterise a family of H-CBFs, and discuss the decision of how many H-CBFs to optimise over in order to find a good LRH-CBF.

A. The Optimisation Problem

The key idea of the proposed approach is to find the optimal choice of CBF with regard to the desired control. To do this, the given CBF $h(\mathbf{x})$ is replaced by a family of CBFs $h(\mathbf{x}, \theta)$ parameterised by $\theta \in \Theta$. Then θ and \mathbf{u} are optimised jointly, to find the H-CBF which enables a safe control \mathbf{u} as close as possible to \mathbf{u}_{des} . Thus, we replace Problem 1 (CBF-QP) with the Least-Restrictive-CBF-Optimisation-Problem (LR-CBF-OP).

Problem 3 (LR-CBF-OP):

$$(\mathbf{u}(\mathbf{x}), \theta) = \underset{\mathbf{u}, \theta}{\operatorname{argmin}} (\mathbf{u} - \mathbf{u}_{\text{des}})^T \mathbf{Q} (\mathbf{u} - \mathbf{u}_{\text{des}}) \quad (16)$$

$$\text{s.t. } \dot{h}(\mathbf{x}, \theta, \mathbf{u}) \geq -\alpha(h(\mathbf{x}, \theta)) \quad (17)$$

$$h(\mathbf{x}, \theta) \geq 0 \quad (18)$$

$$\mathbf{u} \in \mathcal{U}, \theta \in \Theta. \quad (19)$$

Note that we have added line (18) to make sure that the chosen CBF is such that \mathbf{x} is still feasible. This corresponds to removing the hyperplane P_5 in Figure 1, for which the agent and the obstacle are on the same side.

Now this approach can, in principle, be applied to any family of CBFs, but we have chosen H-CBFs since they have closed-form solutions for second-order systems like the double integrator, and the degree of conservativeness has a clear dependence on their orientation. By using the H-CBFs for double integrators in Section III-E, we provide guarantees for both static ($\mathbf{v}_O = 0$) and moving ($\mathbf{v}_O \neq 0$) obstacles. Thus, both cases can be handled, as illustrated in Figure 10.

Remark 1 (Computational Complexity): A key advantage of the CBF approach in general is that Problem 1 is a QP, with a quadratic objective function and linear constraints, which can be solved very efficiently. Looking at Problem 3 above, we note that the objective is still quadratic, but the constraints are not linear in u and θ . One way to address situations where low computational complexity is key is to make Θ a small finite set, having N_θ elements. Then we can pick a fixed $\theta \in \Theta$, and solve Problem 3 (which is a

QP again when θ is fixed). Iterate this over the N_θ different θ , and pick the best solution. In Section V, we explore the performance/computation tradeoff for this approach.

B. Generalisation of the Closest Distance CBF

First, we note that the proposed approach is in fact a generalisation of the very common distance-based CBFs used in [7]–[11]. Let θ_{OH} be the parameter that makes $\hat{\mathbf{n}}(\theta_{OH}) = \hat{\mathbf{n}}_{OA}$, a unit vector aligned with the shortest distance from the obstacle to the agent. Furthermore, let the set Θ be composed of this single element, $\Theta = \{\theta_{OH}\}$. Then, as noted above, Equations (13) and (14) are identical to the ones in [7], and since θ is fixed, Problem 3 is identical to Problem 1. We call this special case OH-CBF.

Given this observation, if the set Θ is chosen such that $\theta_{OH} \in \Theta$, the proposed approach LRH-CBF will never be more restrictive than OH-CBF. Furthermore, as noted above, if Θ is a finite set of N_θ elements, the computations required are N_θ times those of OH-CBF.

C. Existence and Conservativeness

In this section, we will first use results from convex analysis to show when an H-CBF of a given orientation exists, then analyse conservativeness by providing sufficient conditions for when an H-CBF can be found for a given safe trajectory, and provide an example of a very natural safe trajectory that would not be allowed by an OH-CBF.

To investigate some properties of LRH-CBFs, the following two lemmas, inspired by the convex analysis results of Section III-A, state sufficient conditions for safety and conservativeness that are ensured by LRH-CBFs.

Lemma 1: (A H-CBF for each orientation) Given a compact obstacle $O \subset \mathbb{R}^n$ with non-empty interior and a vector $\hat{\mathbf{n}}(\theta)$, there is a H-CBF $h(\mathbf{x}, \theta)$ with normal $\hat{\mathbf{n}}(\theta)$ that is a supporting hyperplane to $\text{conv}(O)$, the convex hull of the obstacle.

Proof: The set $\text{conv}(O)$ is closed, convex, bounded, and has nonempty interior. By Theorem 1 there is a supporting hyperplane with normal $\hat{\mathbf{n}}(\theta)$ that can be turned into a H-CBF $h(\mathbf{x}, \theta)$ using (13) and (14). ■

Lemma 2: (Sufficient conditions for existence of a single H-CBF that does not interfere with a given safe trajectory) Given an obstacle $O \subset \mathbb{R}^n$, and an agent with a trajectory $P = \{p_1, p_2, \dots\} \subset \mathbb{R}^n$ ending at stand still. If the convex hull of the obstacle and the convex hull of the trajectory positions do not intersect, i.e., $\text{conv}(O) \cap \text{conv}(P) = \emptyset$, then there exists a choice θ and α such that the H-CBF $h(\mathbf{x}, \theta)$ would have guaranteed the safety of P .

Proof: By Theorem 2, there exists a hyperplane separating the obstacle from the trajectory. By choosing θ in Lemma 1 such that the normal $\hat{\mathbf{n}}(\theta)$ is equal to the normal of this hyperplane, the H-CBF will also be a separating hyperplane. Since the trajectory ends at a standstill and never intersects the hyperplane, the agent's velocity is always safe from a hyperplane collision point of view, i.e., $h(x) \geq 0$. Now we need to show that (17) is satisfied for the trajectory. Since the trajectory never intersects the hyperplane, we know

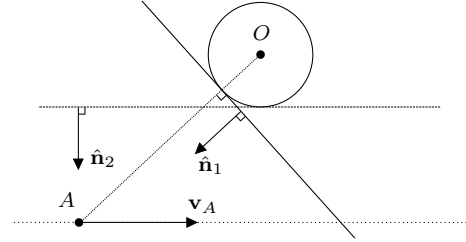


Fig. 2. The geometry of Example 1. The agent A moves along a trajectory with constant velocity \mathbf{v}_A , safely passing the static obstacle O . At the current time, $\hat{\mathbf{n}}_1$ defines a plane orthogonal to the vector connecting A and O , while $\hat{\mathbf{n}}_2$ defines a plane which is parallel to \mathbf{v}_A .

that if $h(x) = 0$ then the corresponding u must have been such that $h(x, u) = 0$, which satisfies (17). If $h(x) > 0$, we can first pick an arbitrary class \mathcal{K}_∞ $\alpha(x)$ function and then choose $\alpha_M(x) = M\alpha(x)$, with $M \in \mathbb{R}$ large enough to satisfy (17) for α_M . ■

Remark 2: Note that Lemma 2 is sufficient for the existence of a *single* H-CBF, while the core idea of the proposed approach is to iteratively find new H-CBFs throughout the execution. Thus, you might imagine a trajectory circling an obstacle, then there would (obviously) not be a single H-CBF proving safety, but the iterative choice of new H-CBFs during the execution could.

The main motivation of this paper is that the LRH-CBF is less conservative than the commonly used OH-CBF, while requiring computations of the same order of magnitude. To support this claim, we first present a detailed example and then a set of simulations.

Example 1: Consider an agent A at position \mathbf{p}_A moving at a velocity \mathbf{v}_A , and a stationary obstacle O at position \mathbf{p}_O , as in Figure 2. Assume that the current desired control is $\mathbf{u}_{\text{des}} = 0$, and that the control is limited by $\|\mathbf{u}\| < u_{\text{max}}$. In Figure 2, A is moving towards O on a trajectory that will not collide with O , as long as $\mathbf{u} = 0$. In regard to the OH-CBF defined by $\hat{\mathbf{n}}_1$, the h -value is given by

$$h(\mathbf{x}) = \hat{\mathbf{n}}_1^T (\mathbf{p}_A - \mathbf{p}_O) - \delta - \frac{(\hat{\mathbf{n}}_1^T \mathbf{v}_A)^2}{2u_{\text{max}}}. \quad (20)$$

Note that if $\|\mathbf{v}_A\|$ is large enough in comparison with u_{max} , the last term will switch the sign of h . Since a state that gives a negative h -value is considered part of the unsafe set, this means that the state of A in Figure 2 is not allowed by an OH-CBF, even though the state is obviously safe. In contrast, the h -value for A in regard to the hyperplane defined by $\hat{\mathbf{n}}_2$ is given by

$$h(\mathbf{x}) = \hat{\mathbf{n}}_2^T (\mathbf{p}_A - \mathbf{p}_O) - \delta. \quad (21)$$

With this choice of halfplane, all magnitudes $\|\mathbf{v}_A\|$ are allowed, as long as the direction of \mathbf{v}_A is given by Figure 2. Note that moving past an obstacle that is still partially in front of an agent, as in this example, is a common situation in environments where the task requires moving close to

obstacles. A simulation of the example above is illustrated in Figures 6 and 7.

In the remainder of this section, we discuss different parameterisations of the H-CBF $h(\mathbf{x}, \theta)$. First, we present the general parametrisation of the H-CBF, then practical details for handling obstacles of arbitrary shape, and finally the special cases of ellipses and circles.

D. H-CBFs for Different Obstacle Shapes

The H-CBF, and in particular $\delta(\theta)$, is obviously dependent on the obstacle shape, but before we go into details we note that the obstacle O below is assumed to be a configuration space obstacle [28] in the sense that it takes the shape of the agent into account (e.g. if the agent has a given radius, the obstacle is inflated by the corresponding amount and the agent considered as a point).

Lemma 3: For a closed, bounded obstacle $O \subset \mathbb{R}^n$, at position P_O , with non-empty interior, we can find an H-CBF (13) with orientation $n(\theta)$ by solving

$$\delta(\theta) = \max_{\mathbf{p} \in \text{conv}(O)} \hat{\mathbf{n}}(\theta)^T \mathbf{p}, \quad (22)$$

where \mathbf{p} is given in a coordinate system centered at \mathbf{p}_O .

Proof: From Theorem 1 we know that there exists a point \mathbf{p}^* and a supporting hyperplane for every direction $\hat{\mathbf{n}}(\theta)$ such that

$$\hat{\mathbf{n}}(\theta)^T \mathbf{p}^* = \max_{\mathbf{p} \in S} \hat{\mathbf{n}}(\theta)^T \mathbf{p} \quad (23)$$

Let $\hat{\mathbf{n}}_{\perp}(\theta)$ be orthogonal to $\hat{\mathbf{n}}(\theta)$, then we can compose \mathbf{p}^* out of two components $\mathbf{p}^* = \delta(\theta)\hat{\mathbf{n}}(\theta) + \gamma(\theta)\hat{\mathbf{n}}_{\perp}(\theta)$, where $\delta(\theta)$ is the distance from \mathbf{p}^* to a hyperplane orthogonal to $\hat{\mathbf{n}}(\theta)$ passing through \mathbf{p}_O . Letting $S = \text{conv}(O)$ and \mathbf{p}^* as above we get $\max_{\mathbf{p} \in \text{conv}(O)} \hat{\mathbf{n}}(\theta)^T \mathbf{p} = \hat{\mathbf{n}}(\theta)^T \mathbf{p}^* = \delta(\theta)$ as above. ■

Remark 3: Note that the optimisation in (22) only needs to be solved once for each θ , for a given obstacle, unlike the optimisation in Problem 3, which is solved each time step.

Lemma 4 (Polygonal Boundaries): For polygonal obstacles, the supporting hyperplane has to intersect at least one vertex, thus the optimisation simplifies to

$$\delta(\theta) = \sup_{\mathbf{p} \in \{p_1, p_2, \dots, p_K\}} \hat{\mathbf{n}}(\theta)^T \mathbf{p}, \quad (24)$$

where $\{p_1, p_2, \dots, p_K\}$ is the vertex set.

Proof: Direct substitution. ■

Lemma 5 (Parameterised Boundaries): If a parameterisation of the boundary of $\text{conv}(O)$ is available in terms of

$$\partial \text{conv}(O) = \{\mathbf{x} | \mathbf{x} = \mathbf{p}_O + \hat{\mathbf{n}}(\phi)r_O(\phi), \phi \in [0, 2\pi)\} \quad (25)$$

where $\mathbf{p}_O \in \text{conv}(O)$, and $r_O : \mathbb{R} \rightarrow \mathbb{R}$ is the radial distance, see Figure 3, then we have

$$\delta(\theta) = \max_{\phi} \{\hat{\mathbf{n}}(\theta)^T \hat{\mathbf{n}}(\phi)r_O(\phi)\}. \quad (26)$$

Proof: Direct substitution. ■

Lemma 6 (Ellipse Boundaries): For an ellipse given in the form

$$\mathbf{r}(\gamma) = [a \cos(\gamma), b \sin(\gamma)], \quad (27)$$

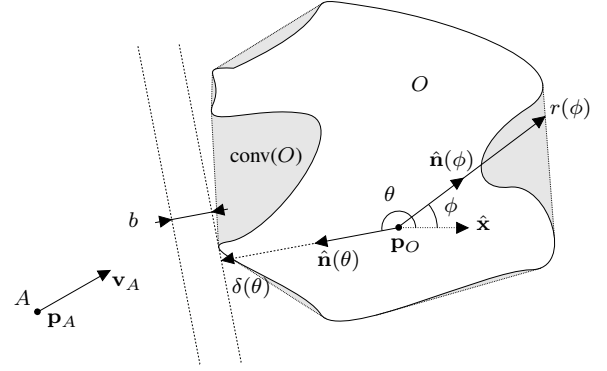


Fig. 3. The geometrics of a general 2D obstacle. The inner white area is the obstacle O , and combined with the light grey areas, we get $\text{conv}(O)$. Notice how the braking distance b added to the supporting hyperplane defines the boundary of the set of safe positions, given the current velocity \mathbf{v}_A .

where a is the major axis, b is the minor axis, and the angle γ is called the eccentric anomaly, the optimisation problem in (26) has the solution

$$\delta(\theta) = a \cos(\theta)\cos(\gamma_{\max}) + b \sin(\theta)\sin(\gamma_{\max}), \quad (28)$$

where $\gamma_{\max} = \arctan 2(b \sin(\theta), a \cos(\theta))$.

Proof: Inserting (27) into (26), we get $\delta(\theta) = \max_{\gamma} \{\hat{\mathbf{n}}(\theta)^T \mathbf{r}(\gamma)\}$. Setting the derivative to zero gives $\frac{\partial}{\partial \gamma} (\hat{\mathbf{n}}(\theta)^T \mathbf{r}(\gamma)) = -\cos(\theta)a \sin(\gamma) + \sin(\theta)b \cos(\gamma) = 0$, which in turn gives the γ_{\max} above, corresponding to (28). ■

The result can be extended to an arbitrary ellipse rotated by an angle β .

E. Closed Form Overapproximations of Delta

If the set of considered orientations Θ of the H-CBF is finite, the expressions above for $\delta(\theta)$ can be precomputed for all $\theta \in \Theta$ for each obstacle. However, if Θ is a continuous interval, you might want a smooth closed-form approximation of $\delta(\theta)$ to avoid computing (22) for each θ .

One way of creating such an approximation that is also periodic (and continuous when θ goes from 2π to 0) is a truncated Fourier series,

$$\tilde{\delta}(\theta) = \frac{a_0}{2} + \sum_{n=1}^N (a_n \cos(n\theta) + b_n \sin(n\theta)) + c, \quad (29)$$

where c is a scalar safety margin making sure the approximation is always an over-approximation, as is needed to guarantee safety.

F. Discrete Time System CBFs

To retain the safety guarantees for discrete-time systems, D-CBFs are needed [27]. The relation between CBFs and D-CBFs, using the h -function in (13), is described in the following lemma:

Lemma 7 (D-CBF): With the h -function in (13), the corresponding D-CBF constraint becomes

$$\dot{h}(\mathbf{x}_k) - \Delta t \frac{(\hat{\mathbf{n}}(\theta)^T (\mathbf{u}_k))^2}{2u_{\max}} \geq -\alpha(h(\mathbf{x}_k)), \quad (30)$$

where $\alpha(x) = x\gamma/\Delta t$, and h and \dot{h} are the same as in the continuous case.

Proof: Calculate the progression of the state after one timestep,

$$\begin{aligned} h(\mathbf{x}_{k+1}) &= h(\mathbf{f}(\mathbf{x}_k) + \mathbf{g}(\mathbf{x}_k)\mathbf{u}_k) \\ &= \hat{\mathbf{n}}(\theta)^T(\mathbf{p}_{A,k} + \Delta t\mathbf{v}_{A,k} - \mathbf{p}_{O,k} - \Delta t\mathbf{v}_{O,k}) \\ &\quad - \delta - \frac{(\hat{\mathbf{n}}(\theta)^T(\mathbf{v}_{A,k} + \Delta t\mathbf{u}_{A,k} - \mathbf{v}_{O,k}))^2}{2u_{\max}} \\ &= h(\mathbf{x}_k) + \Delta t\dot{h}(\mathbf{x}_k) - \frac{(\Delta t\hat{\mathbf{n}}(\theta)^T(\mathbf{u}_k))^2}{2u_{\max}}. \end{aligned} \quad (31)$$

Inserting (31) into (12) results in (30). \blacksquare

Notice how the only difference between the continuous CBF and the D-CBF is the addition of the negative square term. First, this means that the problem reduces to a QCQP for a fixed θ . Secondly, this means that the CBF constraint will be slightly more conservative than a naive Euler approximation of (6), as it decreases the value on the left side.

G. Choosing Θ

The choice of Θ can be made in many ways, but in this section, we provide some observations that might be useful when making a decision. First, it is noted that any $\theta \notin (\theta_{OH} - \pi/2, \theta_{OH} + \pi/2)$ will automatically break the condition (18), since that would render the agent and the obstacle on the same side of the halfplane. In practice, the zone of valid θ choices is even smaller, but it depends on the obstacle size and distance. Second, since θ_{OH} marks the direction of the closest point of the obstacle, it might make sense to pick the rest of the options symmetrically around θ_{OH} . For an infinite Θ , it might thus make sense to pick the interval

$$\Theta = (\theta_{OH} - \pi/2, \theta_{OH} + \pi/2).$$

For a finite Θ , we want to numerically explore the effect of the number of elements N_θ , and the maximum spread, σ_θ , measured from θ_{OH} . Thus we let

$$\Theta_{N_\theta}^{\sigma_\theta} = \{\theta_{OH} - \sigma_\theta, \dots, \theta_{OH}, \dots, \theta_{OH} + \sigma_\theta, \theta_{\text{old}}\}, \quad (32)$$

where the N_θ halfplanes are equally spread between $\theta_{OH} - \sigma_\theta$ and $\theta_{OH} + \sigma_\theta$, and θ_{old} is the previous choice of θ . Note that including θ_{old} gives a recursive safety guarantee. If the last choice of θ and u were safe, then the same θ (i.e. θ_{old}) will have a safe u in this time step, and Problem 3 will have a feasible solution.

V. SIMULATIONS

In this section, the performance of the proposed approach is illustrated through four examples of increasing complexity using a 2D double integrator with actuation constraints. As described above, the contribution of this paper is an approach that has a computational complexity that is very low, and comparable to the highly popular OH-CBF [7]–[11], while giving better performance due to being less restrictive.

Thus, we compare the Continuous and Discrete LRH-CBFs (C- and D-LRH-CBFs) with different choices of Θ , as well as with the OH-CBF from [7]. The simulations are

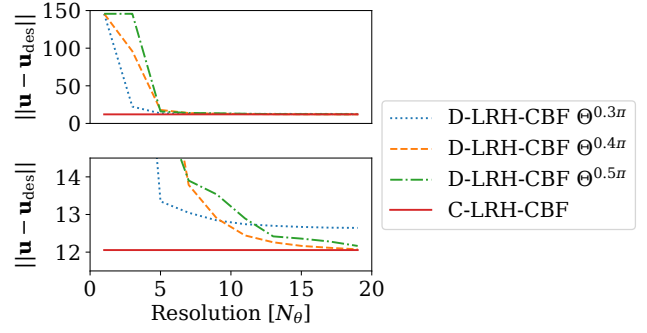


Fig. 4. The aggregate error over 10000 random states in the proximity of a circular obstacle, as a function of N_θ . The continuous solution is used as a baseline, and does not depend on the resolution N_θ . The upper plot shows the full range in $\|\mathbf{u} - \mathbf{u}_{\text{des}}\|$, while the lower shows a zoomed-in version. Note that no improvement is gained when going from $N_\theta = 1$ to $N_\theta = 3$ for $\Theta^{0.5\pi}$, which is an expected result from Section IV-G. Also note that by increasing the resolution from $N_\theta = 1$ quickly decreases $\|\mathbf{u} - \mathbf{u}_{\text{des}}\|$, showing the benefit of LRH-CBF over OH-CBF (the OH-CBF corresponds to $N_\theta = 1$). At resolutions $N_\theta < 9$, a smaller spread of $\Theta^{0.3\pi}$ performs best, while at higher resolutions the wider spread $\Theta^{0.4\pi}$ performs best.

conducted in Python, and continuous numerical optimisation over θ and \mathbf{u} for the C-LRH-CBF is solved using CasADi [29].

Example 2: In this example, the influence of the choice of Θ on the gap $\|\mathbf{u} - \mathbf{u}_{\text{des}}\|$ is investigated. To assess performance, 10000 states and desired controls were randomly sampled in the vicinity of a circular obstacle. Three choices of the spread σ_θ for the D-LRH-CBF were examined over a range of resolutions N_θ , and plotted alongside the solution from the C-LRH-CBF, used as a baseline for comparison. The metrics that were considered were the aggregated error $\|\mathbf{u} - \mathbf{u}_{\text{des}}\|$ and the mean computation time over 10000 samples. The results are presented in Figures 4 and 5. From Figure 4, it is apparent that a significant improvement is achieved when increasing the resolution with only a few halfplanes. This implies that without much additional computational time, the difference $\|\mathbf{u} - \mathbf{u}_{\text{des}}\|$ is greatly reduced compared to the OH-CBF (which corresponds to $N_\theta = 1$). Looking at the zoomed-in performance in the lower part of Figure 4, it is apparent that the choice of σ_θ has a major impact on convergence with the continuous solution. While a small spread $\sigma_\theta = 0.3\pi$ is good for resolutions $N_\theta \leq 9$, better performance is achieved with $\sigma_\theta = 0.4\pi$ for resolutions $N_\theta > 9$. The time complexity, shown in Figure 5, is linear in the choice of N_θ , as expected. We also note that the approach is indeed quite fast, using an Intel Core Ultra 9 185H with WSL, the time per step is approximately $6.8N_\theta \times 10^{-6}$ s. For the continuous solution, each step takes about 7.2×10^{-3} s.

Example 3: In this example, which is a numerical version of Example 1, the agent moves on a safe straight line with constant velocity, passing a static obstacle, as seen in Figure 6. Parts of the path are, however, *not considered safe* (feasible) with respect to an OH-CBF, as seen in Figure 7. For $t \in [1.5, 2.2]$, the h -value is negative, which means that

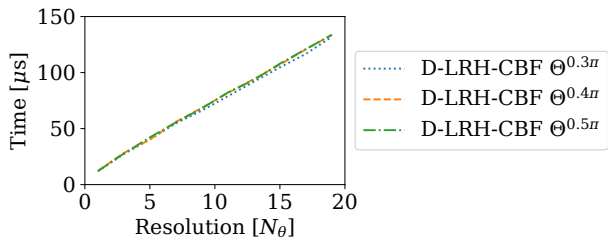


Fig. 5. The mean computational time over 10000 steps as a function of N_θ . At max resolution, $N_\theta = 19$, a step takes about $130 \mu\text{s}$. As the relationship between time and N_θ is linear and independent of σ_θ , the expected time of a single step is approximately $6.8N_\theta \mu\text{s}$. The mean time to solve a step with the continuous solver is 7.2 ms , too long to be shown in the same plot.

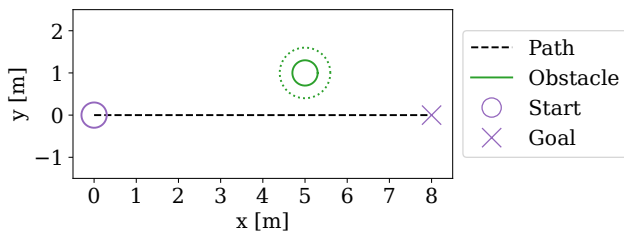


Fig. 6. The setup of example 3. The agent moves on a straight line at constant velocity ($\mathbf{u}_{\text{des}} = 0$), safely passing an obstacle (the dotted circle corresponds to the configuration space of the obstacle). The corresponding h -value for the four different cases is shown in Figure 7.

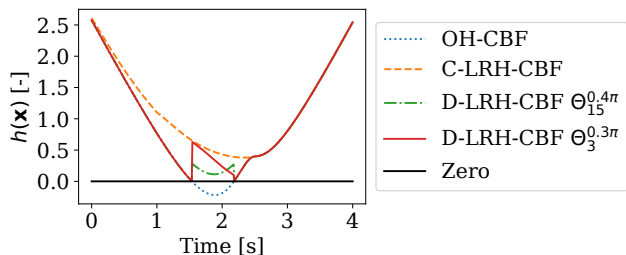


Fig. 7. The h -value for the fixed trajectory of the agent in Example 3. Note that this safe trajectory would not be allowed by the OH-CBF of [7] (dotted), as the h -value is negative for $t \in [1.5, 2.2]$, right before passing the obstacle. This is independent of the choice of α . However, since the h -value is positive during the entire trajectory for both the discrete and continuous implementations of the LRH-CBF (dashed, dash-dotted, and solid), there exists an α that allows the trajectory. Note that some of the LRH-CBFs only deviate from the OH-CBF when it is needed (to avoid restricting the control), i.e., when the h -value of OH-CBF turns negative around $t = 1.5$.

the state is considered unsafe. No matter the choice of α , this safe trajectory can not be followed using an OH-CBF. In contrast, the h -value for a set of LRH-CBFs remains above zero throughout the trajectory, which implies that the trajectory can be followed given the right choice of α . This shows that by optimising over θ , the resulting H-CBF is indeed less restrictive.

Example 4: In this example, the OH-CBF and LRH-CBFs are compared to each other in a scenario with a single static obstacle blocking the direct path to the goal, as seen in Figure 8, with corresponding data in Figure 9. The agent

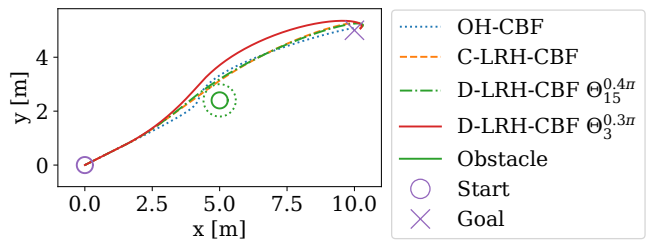


Fig. 8. The setup of example 4. The agent is driven towards the goal with a PD-controller, using the two types of H-CBFs. Note how all the LRH-CBFs leave the direct path to the goal early with a small correction of the path, while the OH-CBF results in an early and significant slowdown, and then turns closer to the obstacle. As can be seen in Figure 9, the OH-CBF actually starts slowing down before the LRH-CBFs start turning. This is expected, as the LRH-CBFs are searching for a θ that minimises $\|\mathbf{u} - \mathbf{u}_{\text{des}}\|$.

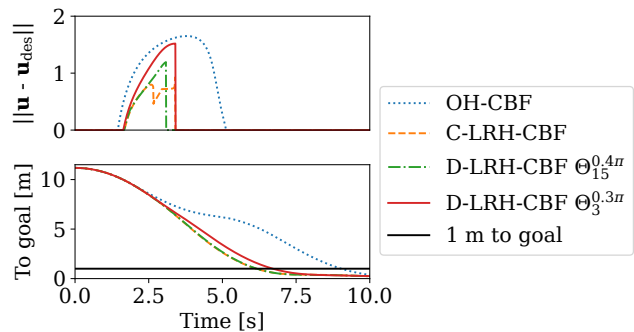


Fig. 9. Upper: The difference between the desired control and the safe control $\|\mathbf{u} - \mathbf{u}_{\text{des}}\|$ over time. The OH-CBF comes into effect earlier and for a longer time, compared to three implementations of the LRH-CBF. Lower: The distance to the goal as a function of time. The OH-CBF is slowest, and arrives within 1 m of the goal in 9.0 s, while the three LRH-CBFs do so between 6.1 and 7 s.

starts at rest and is driven by a PD-controller that provides \mathbf{u}_{des} . As can be seen from $\|\mathbf{u} - \mathbf{u}_{\text{des}}\|$ in Figure 9 (upper), the OH-CBF starts to restrict acceleration earlier than the LRH-CBFs, enforces a larger gap $\|\mathbf{u} - \mathbf{u}_{\text{des}}\|$, and does so for a longer time. Furthermore, looking at the trails of the paths in Figure 8, we see that the OH-CBF drives straight forward for longer, while slowing down, and starts turning fairly late, while the LRH-CBFs leaves the direct path earlier, maintains a higher speed (slope of goal distance plot), and arrives at the goal much sooner. The performance of the discrete and continuous LRH-CBFs is very similar.

Example 5: In this example, the agent encounters two static polygon-shaped obstacles, as well as an ellipse moving at constant velocity. The results for both the OH-CBF and the LRH-CBF are shown in Figure 10. Notice how the LRH-CBF enables the agent to move closer to the obstacles, and at a greater velocity compared to the OH-CBF.

VI. CONCLUSION

In all earlier work, the CBF is chosen before it is time to find a safe control. In this paper, we suggest selecting the CBF with the desired control in mind. This way, we can

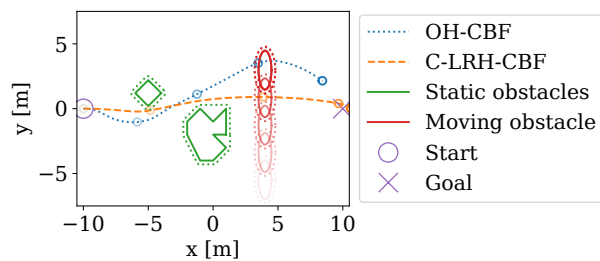


Fig. 10. The trajectories in Example 5, featuring moving and irregularly shaped obstacles. Concurrent snapshots of the agent and the moving obstacle are shown, with older ones increasingly opaque. Notice how the LRH-CBF is less conservative regarding the obstacles, resulting in a faster trajectory.

find the least restrictive CBF with respect to what we want to achieve. The advantages of the proposed approach were illustrated in five examples, including moving obstacles.

REFERENCES

- [1] S. Prajna, A. Jadbabaie, and G. J. Pappas, "A Framework for Worst-Case and Stochastic Safety Verification Using Barrier Certificates," *IEEE Transactions on Automatic Control*, vol. 52, no. 8, pp. 1415–1428, Aug. 2007.
- [2] A. D. Ames, J. W. Grizzle, and P. Tabuada, "Control barrier function based quadratic programs with application to adaptive cruise control," in *53rd IEEE Conference on Decision and Control*, Dec. 2014, pp. 6271–6278.
- [3] A. D. Ames, S. Coogan, M. Egerstedt, G. Notomista, K. Sreenath, and P. Tabuada, "Control Barrier Functions: Theory and Applications," in *2019 18th European Control Conference (ECC)*, Jun. 2019, pp. 3420–3431.
- [4] K.-C. Hsu, H. Hu, and J. F. Fisac, "The Safety Filter: A Unified View of Safety-Critical Control in Autonomous Systems," *Annual Review of Control, Robotics, and Autonomous Systems*, vol. 7, no. 1, pp. 47–72, Jul. 2024.
- [5] Y. Chen, M. Jankovic, M. Santillo, and A. D. Ames, "Backup Control Barrier Functions: Formulation and Comparative Study," Apr. 2021, arXiv:2104.11332 [eess].
- [6] H. Yu, C. Hirayama, C. Yu, S. Herbert, and S. Gao, "Sequential Neural Barriers for Scalable Dynamic Obstacle Avoidance," in *2023 IEEE/RSSJ International Conference on Intelligent Robots and Systems (IROS)*, Oct. 2023, pp. 11 241–11 248.
- [7] U. Borrmann, L. Wang, A. D. Ames, and M. Egerstedt, "Control Barrier Certificates for Safe Swarm Behavior," *IFAC-PapersOnLine*, vol. 48, no. 27, pp. 68–73, Jan. 2015.
- [8] L. Wang, A. D. Ames, and M. Egerstedt, "Safety Barrier Certificates for Collisions-Free Multirobot Systems," *IEEE Transactions on Robotics*, vol. 33, no. 3, pp. 661–674, Jun. 2017.
- [9] T. G. Molnar, S. K. Kannan, J. Cunningham, K. Dunlap, K. L. Hobbs, and A. D. Ames, "Collision Avoidance and Geofencing for Fixed-Wing Aircraft With Control Barrier Functions," *IEEE Transactions on Control Systems Technology*, vol. 33, no. 5, pp. 1493–1508, Sep. 2025.
- [10] R. Funada, K. Nishimoto, T. Ibuki, and M. Sampei, "Collision Avoidance for Ellipsoidal Rigid Bodies With Control Barrier Functions Designed From Rotating Supporting Hyperplanes," *IEEE Transactions on Control Systems Technology*, vol. 33, no. 1, pp. 148–164, Jan. 2025.
- [11] E. H. Thyri, E. A. Basso, M. Breivik, K. Y. Pettersen, R. Skjetne, and A. M. Lekkas, "Reactive collision avoidance for ASVs based on control barrier functions," in *2020 IEEE Conference on Control Technology and Applications (CCTA)*, Aug. 2020, pp. 380–387.
- [12] S. Liu, Y. Mao, and C. A. Belta, "Safety-Critical Planning and Control for Dynamic Obstacle Avoidance Using Control Barrier Functions," in *2025 American Control Conference (ACC)*, Jul. 2025, pp. 348–354.
- [13] P. Tooranjipour and B. Kiumarsi, "LiDAR-based Model Predictive Control using Control Barrier Functions," in *2025 American Control Conference (ACC)*, Jul. 2025, pp. 315–322.
- [14] A. Thirugnanam, J. Zeng, and K. Sreenath, "Safety-Critical Control and Planning for Obstacle Avoidance between Polytopes with Control Barrier Functions," in *2022 International Conference on Robotics and Automation (ICRA)*, May 2022, pp. 286–292.
- [15] S. Wu, Y. Fang, N. Sun, B. Lu, X. Liang, and Y. Zhao, "Optimization-Free Smooth Control Barrier Function for Polygonal Collision Avoidance," *IEEE Transactions on Cybernetics*, vol. 55, no. 9, pp. 4257–4269, Sep. 2025.
- [16] S. Wei, R. Khorrambakht, P. Krishnamurthy, V. Mariano Gonçalves, and F. Khorrani, "Collision Avoidance for Convex Primitives via Differentiable Optimization-Based High-Order Control Barrier Functions," *IEEE Transactions on Control Systems Technology*, pp. 1–16, 2025.
- [17] G. Notomista, G. P. T. Choi, and M. Saveriano, "Reactive Robot Navigation Using Quasi-Conformal Mappings and Control Barrier Functions," *IEEE Transactions on Control Systems Technology*, vol. 33, no. 3, pp. 928–939, May 2025.
- [18] B. Dai, R. Khorrambakht, P. Krishnamurthy, V. Gonçalves, A. Tzes, and F. Khorrani, "Safe Navigation and Obstacle Avoidance Using Differentiable Optimization Based Control Barrier Functions," *IEEE Robotics and Automation Letters*, vol. 8, no. 9, pp. 5376–5383, Sep. 2023, arXiv:2304.08586 [cs].
- [19] A. Ghaffari, I. Abel, D. Ricketts, S. Lerner, and M. Krstic, "Safety Verification Using Barrier Certificates with Application to Double Integrator with Input Saturation and Zero-Order Hold," in *2018 Annual American Control Conference (ACC)*. Milwaukee, WI: IEEE, Jun. 2018, pp. 4664–4669.
- [20] J. Huang, J. Zeng, X. Chi, K. Sreenath, Z. Liu, and H. Su, "Dynamic Collision Avoidance Using Velocity Obstacle-Based Control Barrier Functions," *IEEE Transactions on Control Systems Technology*, vol. 33, no. 5, pp. 1601–1615, Sep. 2025.
- [21] A. S. Roncero, R. I. C. Muchacho, and P. Ögren, "Multi-Agent Obstacle Avoidance using Velocity Obstacles and Control Barrier Functions," Mar. 2025, arXiv:2409.10117 [cs].
- [22] L. An and G.-H. Yang, "Collisions-Free Distributed Optimal Coordination for Multiple Euler-Lagrangian Systems," *IEEE Transactions on Automatic Control*, vol. 67, no. 1, pp. 460–467, Jan. 2022.
- [23] X. Tan and D. V. Dimarogonas, "Distributed Implementation of Control Barrier Functions for Multi-agent Systems," *IEEE Control Systems Letters*, vol. 6, pp. 1879–1884, 2022.
- [24] D. Martínez-Baselga, E. Sebastián, E. Montijano, L. Riazuelo, C. Sagüés, and L. Montano, "AVOCADO: Adaptive Optimal Collision Avoidance Driven by Opinion," *IEEE Transactions on Robotics*, vol. 41, pp. 2495–2511, 2025.
- [25] M. A. Abbas, R. Milman, and J. M. Eklund, "Obstacle Avoidance in Real Time With Nonlinear Model Predictive Control of Autonomous Vehicles," *Canadian Journal of Electrical and Computer Engineering*, vol. 40, no. 1, pp. 12–22, 2017.
- [26] T. Rockafellar, *Convex Analysis*. Princeton University Press, 1970.
- [27] A. Agrawal and K. Sreenath, "Discrete Control Barrier Functions for Safety-Critical Control of Discrete Systems with Application to Bipedal Robot Navigation," in *Robotics: Science and Systems XIII*, Jul. 2017.
- [28] S. M. LaValle, *Planning Algorithms*, 1st ed. Cambridge University Press, May 2006.
- [29] J. A. E. Andersson, J. Gillis, G. Horn, J. B. Rawlings, and M. Diehl, "CasADi: a software framework for nonlinear optimization and optimal control," *Mathematical Programming Computation*, vol. 11, no. 1, pp. 1–36, Mar. 2019.